Hindawi Publishing Corporation
International Journal of Photoenergy
Volume 2015, Article ID 592308, 13 pages
http://dx.doi.org/10.1155/2015/592308

Review Article

Perovskite Solar Cells: Potentials, Challenges, and Opportunities

Muhammad Imran Ahmed,[1] Amir Habib,[1] and Syed Saad Javaid[2]

[1]*School of Chemical and Materials Engineering, National University of Sciences and Technology, Islamabad 44000, Pakistan*
[2]*College of Aeronautical Engineering, National University of Sciences and Technology, Islamabad 44000, Pakistan*

Correspondence should be addressed to Muhammad Imran Ahmed; imranrahbar@scme.nust.edu.pk

Received 16 March 2015; Revised 30 May 2015; Accepted 1 July 2015

Academic Editor: Shuping Pang

Copyright © 2015 Muhammad Imran Ahmed et al. This is an open access article distributed under the Creative Commons Attribution License, which permits unrestricted use, distribution, and reproduction in any medium, provided the original work is properly cited.

Heralded as a major scientific breakthrough of 2013, organic/inorganic lead halide perovskite solar cells have ushered in a new era of renewed efforts at increasing the efficiency and lowering the cost of solar energy. As a potential game changer in the mix of technologies for alternate energy, it has emerged from a modest beginning in 2012 to efficiencies being claimed at 20.1% in a span of just two years. This remarkable progress, encouraging at one end, also points to the possibility that the potential may still be far from being fully realized. With greater insight into the photophysics involved and optimization of materials and methods, this technology stands to match or even exceed the efficiencies for single crystal silicon solar cells. With thin film solution processability, applicability to flexible substrates, and being free of liquid electrolyte, this technology combines the benefits of Dye Sensitized Solar Cells (DSSCs), Organic Photovoltaics (OPVs), and thin film solar cells. In this review we present a brief historic perspective to this development, take a cognizance of the current state of the art, and highlight challenges and the opportunities.

1. Introduction

Solar energy, along with wind, biomass, tidal, and geothermal energy, is emerging as an alternate source of energy for our energy-starved planet. Out of the mix, solar energy is the most abundant and clean form of energies offering an answer to the increasing concern of global warming and greenhouse gases by fossil fuels. Over the past four decades silicon solar cells have advanced tremendously both in terms of cost of production and efficiency [1, 2]. In some locations of the world they are delivering on grid power at competitive costs compared to that of fossil fuels. Newer in the mix in the form of thin film and vapor deposited semiconductor based technologies, like CdTe or CIGS [3, 4], and organic/inorganic solar cells, hybrid composites or inorganic semiconductors [5–10], referred to as second and third generation solar cells, are pushing the frontiers further in terms of ease of processing, cost, efficiency, and stability owing to sustained research effort over the last decade. This has resulted in the availability of commercial products from this line of solar cells to select consumers in power electronics and low power applications in buildings. However, for their adoption in larger markets, the per watt cost has to be brought down to a level comparable to that of electricity generated from fossil fuels. This demands a substantial increase in efficiency and cost reduction for these emerging technologies. Recent advances in the manufacturing of main stream silicon solar cell assure incorporation of photovoltaics in main stream energy mix, with a recent forecast anticipating a third of the global electricity demand being met by photovoltaics by 2030 [1].

Silicon based solar cell technologies offering a combination of properties, like ease of surface passivation, low cost, hardness, and high temperature stability, have made themselves a favored option in photovoltaic applications. Technologies promising a combination of lower cost and ease of fabrication with a better energy payback matrix offer exciting opportunities for replacement of silicon. As new entrant in this field, organometallic halide perovskites offer captivation prospects [11–14]. Solution processability, broad spectrum solar absorption, low nonradiative recombination losses, and the potential to capitalize on over two decades of research and development in the field of dye sensitized and organic solar cells provide all the right ingredients for this

technology to prove a viable alternate to the dominance of silicon. The efficiency for this class of solar cells has jumped from a meager 3.9% in 2009 to over 15% in 2013 on the back of properties like high absorption coefficient, panchromatic absorption, low exciton binding energies, longer diffusion lengths and lifetimes, and the range of options as to composition and preparation.

In this review, we present the current state of the art for photovoltaic devices based on perovskites, spelling out the underlying phenomenon, different device architectures, fabrication techniques, comparison to other technologies, and future outlook and challenges. This paper is aimed at recollecting the recent developments in perovskite solar cells, providing a broader context to the reviews already published on this topic [11, 15–17].

2. The Phenomena

Perovskites are a family of materials with the crystal structure of calcium titanate, that is, ABX_3. There are numerous materials which adopt this structure with exciting applications based on thermoelectric, insulating, semiconducting, piezoelectric, conducting, antiferromagnetic, and superconducting properties [19]. Perovskites are routinely synthesized by solid-state mixing of constituent elements or compounds at high temperatures in the range of >1300 K [20]. They can also be synthesized by drying the solution of precursor salts and the ones offering semiconductor properties find important applications in printable electronics due to solution processability [21, 22].

ABX_3 describes the crystal structure of perovskite class of materials, where A and B are cations and X is an anion of different dimensions with A being larger than X. Crystal structure of perovskites is illustrated in Figure 1. Considerations of tolerance factor **t** and octahedral factor $\boldsymbol{\mu}$ [23] dictate probable structure and crystallographic stability where **t** is defined by the ratio of the bond length A–X to that of B–X in an ideal solid sphere model ($\mathbf{t} = (rA + rX)/\{\sqrt{2}(rB + rX)\}$, where rA, rB, and rX are the ionic radii involved) and the ratio rB/rX defines the octahedral factor $\boldsymbol{\mu}$. $0.81 < \mathbf{t} < 1.11$ and $0.44 < \boldsymbol{\mu} < 0.90$ [23] are the typical values for halide perovskites (X = F, Cl, Br, and I). Narrower range of **t** values form 0.89 to 1.0 dictates cubic structure, while lower values of **t** stabilize less symmetric tetragonal and orthorhombic structures. In organic inorganic halide perovskite of interest in photovoltaic applications, A is a larger organic cation typically methylammonium ($CH_3NH_3^+$) with rA = 0.18 nm [24], though good results have also been reported for ethylammonium ($CH_3CH_2NH_3^+$) (rA = 0.23 nm) [25–28] and formamidinium ($NH_2\ CH{=}NH_2^+$) (rA is estimated in the range 0.19–0.22 nm) [29–31]. Anion X is a halogen, typically iodine (rX = 0.220 nm), though Br and Cl are also increasingly being reported (rX = 0.196 nm and 0.181 nm), typically in a mixed halide configuration. Pb (rB = 0.119 nm) and Sn (rB = 0.110 nm), as cation B, have exclusively been used for high efficiency perovskite solar cells because of lower and theoretically ideal band gaps [29]. Lower stability associated with Sn is due to ease of oxidation of Sn to SnI_4 while relativistic effects afford greater oxidation protection in Pb [29]. Thus the standard compound is methylammonium lead triiodide ($CH_3NH_3PbI_3$), with mixed halides $CH_3NH_3PbI_{3-x}Cl_x$ and $CH_3NH_3PbI_{3-x}Br_x$ also being important.

3. Perovskite-Sensitized Solar Cells

DSSCs [7, 32] are the forerunners of perovskite solar cells. Constituent of a typical DSSC is mesoporous n-type titania sensitized with a light absorbing dye in a redox active electrolyte. Porous titania affords greater internal surface area to the sensitized dye for efficient absorption of incident photons though thicker films of the order of 10 μm are required for complete absorption over the absorbing range of the dye [32]. The requirement of 10 μm thick active layer is impractical for solid-state DSSCs where a number of factors limit the active layer thickness to less than 2 μm [33]. As an alternate, thin film semiconductor active layers and quantum dots enable complete light absorption in much thinner layers while at the same time pushing the photosensitivity further into near infrared (NIR) [34–38]. In the backdrop of finding more efficient light sensitizers for DSSCs, Miyasaka and coworkers reported the first perovskite-sensitized solar cells between 2006 and 2008. $CH_3NH_3PbI_3$ and $CH_3NH_3PbBr_3$ absorbers were employed with an iodide triiodide redox couple or a polypyrrole carbon black composite solid-state hole conductor. Full sun power conversion efficiency varying between 0.4 and 2% was measured for solid-state and liquid electrolyte cells, respectively [39, 40].

The first peer-reviewed report for perovskite-sensitized solar cell was published in 2009; $CH_3NH_3PbI_3$ absorber in an iodide/triiodide redox couple achieved an efficiency of 3.5% [41]. Figure 2 illustrates the schematic of an organometallic halide sensitized titania solar cell and the associated spectral response. Retaining the liquid electrolyte reported by Kim and coworkers achieved an improved efficiency of 6.5% by optimizing the titania surface morphology and perovskite processing [41, 42]. The tumbling block in the liquid electrolyte based perovskite-sensitized solar cell was the dissolution and decomposition of perovskite in the liquid electrolyte. Resultantly the solar cells exhibited poor stability and would degrade within minutes [41, 42]. The solution to this problem lied in adoption of solid-state hole transport medium in place of electrolyte as was originally tried by Kojima and coworkers in 2006 [40]. Methylammonium trihalogen plumbates, being relatively insoluble in nonpolar organic solvents, paved the way for realizing first perovskite sensitization and made subsequent infilling with the organic hole conductor possible. This made T. N. Murakami and T. Miyasaka and N. G. Park in collaboration with M. Grätzel and coworkers develop solid-state perovskite solar cells employing (2,2(7,7)-tetrakis-(N,N-dipmethoxyphenylamine)9,9(-spirobifluorene)) (spiro-MeOTAD) as the hole transporter [43] with maximum full sun power conversion efficiencies of between 8 and 10% employing $CH_3NH_3PbI_{3-x}Cl_x$ mixed halide perovskite and $CH_3NH_3PbI_3$, respectively [18, 44].

This achievement marked a considerable jump in performance over the best reported solid-state (ss) DSSCs with a

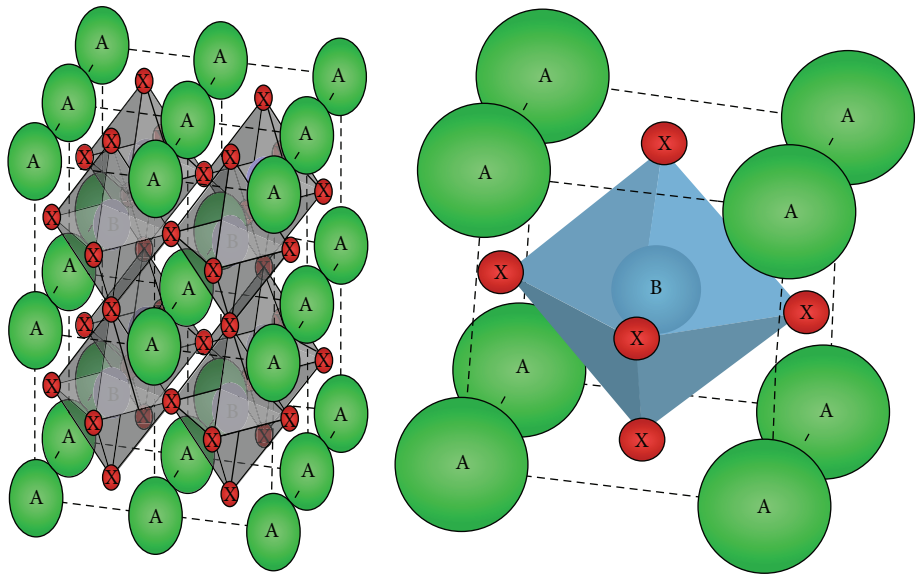

Figure 1: Perovskite crystal structure.

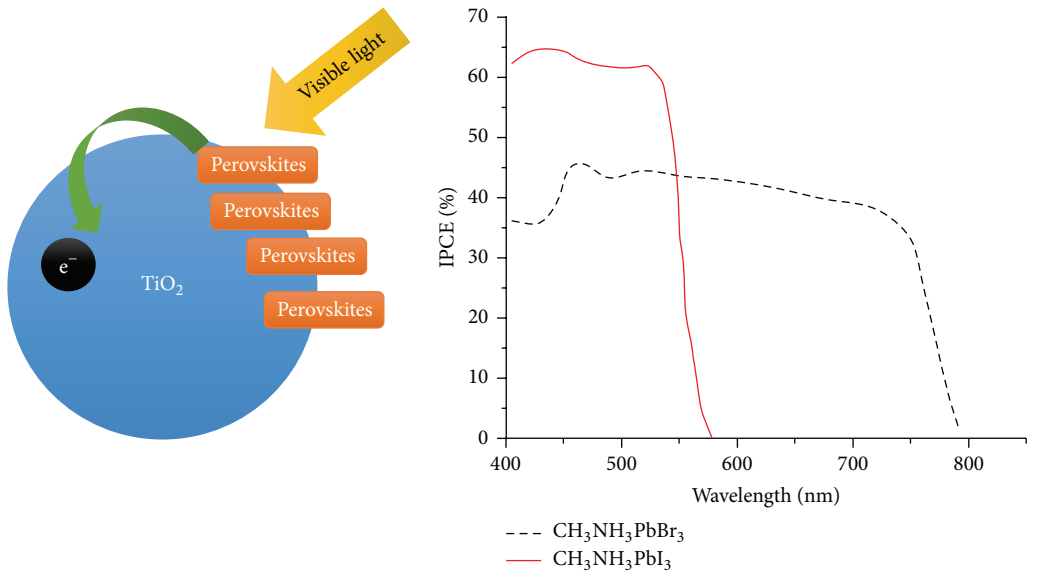

Figure 2: Schematic of perovskite-sensitized TiO_2 undergoing photoexcitation and electron transfer (left). The incident photon-to-electron conversion efficiency (IPCE) spectra for perovskite-sensitized solar cells [18].

recorded efficiency of over 7% [45]. This is made possible by the advantages perovskites afford over conventional dyes in the form of stronger absorption over a broader range resulting in complete absorption in film thickness as low as 500 nm. This is a considerable advantage for solid-state cells where light absorption and photocurrent generation have typically been limited by the requirement of film thickness of around 2 μm [33].

4. Mesoporous TiO_2 Scaffold

First reported high efficiency and stable perovskite solar cell [46] was synthesized by spin coating γ-butyrolactone solution containing equimolar CH_3NH_3I and PbI_2 in 2012. This resulted in deposition of semispherical nanodots of $CH_3NH_3PbI_3$ on TiO_2. Since the surface was not fully covered with nanodots it was evident that photoexcited electrons were transferred from $CH_3NH_3PbI_3$ to TiO_2. This cell with a 0.6 μm titania film achieved a PCE of 9.7% and a Voc of 888 mV. Fill factor of 0.62 was indicative of poor pore filling with spiro-MeOTAD and resulting poor interface between Hole Transport Material (HTM), active layer, and Electron Transport Material (ETM).

A device architecture of $TiO_2/CH_3NH_3PbI_3$/Au [41] experimentally confirmed the hole transport properties of $CH_3NH_3PbI_3$. It achieved a PCE of 5.5% with FTO/100 nm

thick TiO_2 as hole blocking and electron-transporting material. Increase of TiO_2 to 100 nm improved PCE to 8% [47]. Mott-Schottky analysis was used to confirm depletion zone between TiO_2 and $CH_3NH_3PbI_3$, and the structure was referred to as depleted heterojunction perovskite solar cell. Large shunt resistance caused a poor fill factor (FF) and a lower External Quantum Efficiency (EQE) at long wavelength range of 540–800 nm.

Ambipolar characteristics of $CH_3NH_3PbI_3$ were reported by Laban and Etgar [48], based on thin film transistor (TFT) analysis, with slightly stronger p-type nature. Static and transient photoluminescence (PL) decay studies established that charge carriers are injected into TiO_2 with some charge separation taking place at $CH_3NH_3PbI_3$/poly(triarylamine) HTM interface as well. Superior PCE over spiro-MeOTAD system is attributed to thin (~30 nm) HTM layer as compared to spiro-MeOTAD HTM (~500 nm) resulting in reduced series resistance. Devices without HTM exhibited poor performance necessitating a physiochemical study of $CH_3NH_3PbI_3$ systems.

Perovskite light harvesters have also been reported with one-dimensional nanostructures. Rutile TiO_2 (~0.6 μm long) with photoactive $CH_3NH_3PbI_3$ achieved PCE of 9.4% [49]. Increasing the length from 0.6 to 1.6 μm decreased the photovoltaic performance. With an increase in the length of nanorods, the tilted nanorods resulted in problems in pore filling with spiro-MeOTAD. A change from nanodot deposition of active layer to pillared structure can overcome this issue. Br–I mixed perovskite $CH_3NH_3PbI_2Br$ with TiO_2 achieved PCE of 4.87%, slightly higher than that achieved for $CH_3NH_3PbI_3$ owing to the higher Voc of $CH_3NH_3PbI_2Br$ mixed halide perovskite [50].

$CH_3NH_3PbBr_3$ in a mesoporous TiO_2 with poly[N-9-hepta-decanyl-2,7-carbazole-alt-3,6-bis-(thiophen-5-yl)-2,5-dioctyl-2,5-dihydropyrrolo[3,4-]pyrrole-1,4-dione] (PCBTDPP) as HTM layer generated a Voc of 1.2 V [51]. With P3HT used as HTM, Voc reduced to 0.5 V. When considering electron injection from the photoactive layer to mesoporous titania, Voc is determined by difference in the Fermi level of TiO_2 and the HOMO level of the HTM. Such large difference in Voc while the HOMO levels are only 0.02 eV apart in PCBTCP and P3HT (PCBTDPP: 5.4 eV and P3HT: 5.2 eV) was attributed to the efficiency of light filtering and degree of chemical interaction [52]. PCBTDPP based device afforded enhanced light filtering and stronger chemical interaction effecting charge recombination and an up-shift of Fermi level resulting in a high Voc. Faster recombination in P3HT resulted in electron lifetime being one order of magnitude lower than spiro-MeOTAD in TiO_2/$CH_3NH_3PbI_3$/HTM system [53]. These results suggest that factor other than energy levels must be born in mind for selecting HTMs.

5. Mesosuperstructured PSCs Based on Nonelectron Injecting Oxides

$CH_3NH_3PbI_2Cl$ mixed perovskite coated alumina layer in a photovoltaic cell resulted in a PCE of 10.9% [54]. This device structure was called "mesosuperstructured solar cell" (MSSC) as the photogenerated electrons are not transferred to alumina because of the difference in band edges of alumina and perovskite active layer, which acts only as a scaffold for carrying the photoactive layer. Spin coated $CH_3NH_3PbI_2Cl$ was more stable in air than $CH_3NH_3PbI_3$. Smaller size of Cl^- ion presumably stabilizes the anion in perovskite structure. Al_2O_3–$CH_3NH_3PbI_2Cl$ system generated higher Voc than TiO_2–$CH_3NH_3PbI_2Cl$. Photoinduced spectroscopic study confirmed that the difference is due to the differing behavior of photogenerated electrons in the two systems. Scaffold layers afford processing at lower temperatures by excluding high temperatures annealing step as neither are generated electrons injected into the mesoporous layer nor transported. PCE value of 12.3% [33] was achieved for the low temperature processed mesosuperstructured solar cell (as 150°C-dried Al_2O_3 mesoporous layers). Varying the thickness of the Al_2O_3 scaffold layer from 0 (no scaffold) to ca. 400 nm, a perovskite $CH_3NH_3I_{3-x}Cl_x$ overlayer formed on the 80 nm thick alumina film, though no capping layer formed on the 400 nm thick Al_2O_3 film. The highest PCE was observed from the 80 nm Al_2O_3 layer resulting in highest Jsc, while 400 nm Al_2O_3 layer exhibited improved Voc and FF. These results suggest that enhanced crystallinity in perovskite active layer enhances Jsc, while pinhole-free perovskite results in high Voc and FF. Codeposited alumina nanoparticle suspension (5 wt% Al_2O_3) and perovskite precursors in DMF resulted in a PCE of 7.16% [55].

CH_3NH_3-$PbBr_3$ with a larger bandgap (E_g = 2.3 eV) than $CH_3NH_3PbI_3$ was employed as a light harvester and electron transporter employing the mesosuperstructure concept. Voc of 1.3 V [56] was achieved with device structure of Al_2O_3/$CH_3NH_3PbBr_3$/N,N′-dialkylperylene diimide (PDI). This large Voc could be explained due to the large difference between LUMO (4.2 eV) of CH_3NH_3-$PbBr_3$ and the HOMO (5.8 eV) of PDI and the noninjection of photoexcited electrons into the alumina scaffold. Mesosuperstructure concept was also evaluated with ZrO_2 mesoporous scaffold with $CH_3NH_3PbI_3$ light harvester exhibiting significant photovoltaic activity Voc of ~900 mV though lower than titania [57]. Impedance spectroscopic study employing three-electrode electrochemical cell verified that zirconia scaffold was not charged up to a bias of 0.9 V in contrast to titania mesoporous layer indicating that the photogenerated electrons are not injected into zirconia scaffold [57]. This comparative study determined that $CH_3NH_3PbI_3$ was able to accumulate charges owing to large density of states (DOS). A higher efficiency of 10.8% was reported for CH_3-NH_3PbI_3 [51], sensitizing ZrO_2 scaffold with a Voc of 1.07 V.

6. Planar Heterojunction Structured Cells

Thermally coevaporated CH_3NH_3I and $PbCl_2$ and deposited $CH_3NH_3PbI_{3-x}Cl_3$ onto FTO with a thin TiO_2 layer resulted in a PCE of 15.4% [58]. This proves the bifunctional property of perovskites, that is, photoexcitation and charge transport. Mesoporous oxide layer thus may not be required. Vapor deposited perovskite layer showed an enhanced PCE over solution processed active layer due to increased morphology control and formation of homogeneous flat, pinhole-free active layer. While it is easier to obtain a flat

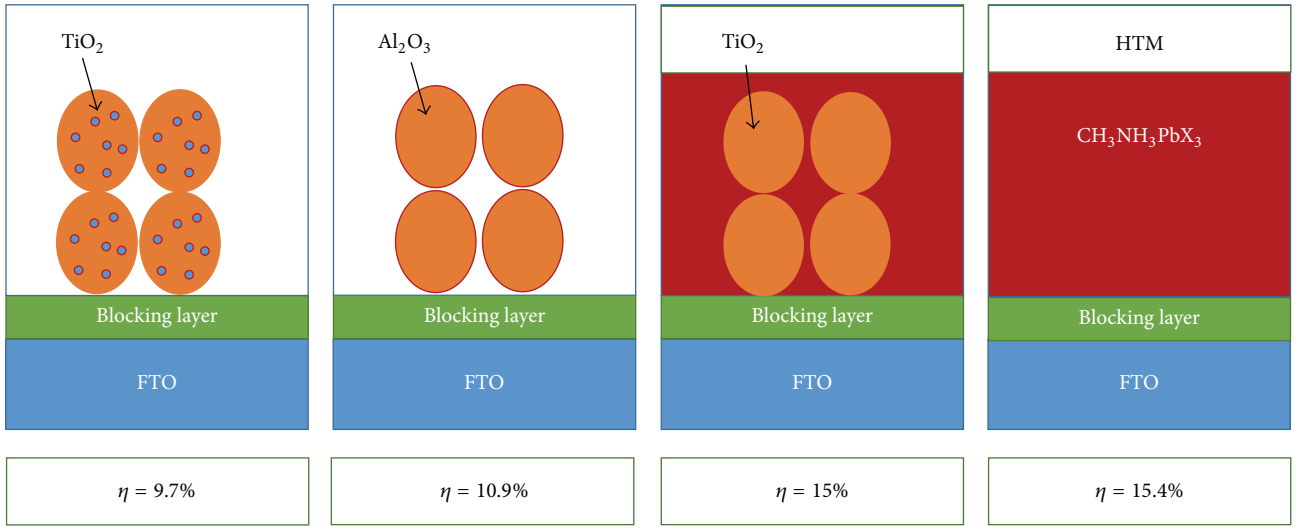

Figure 3: Progress in perovskite solar cells, from PCE of 9.7% through 10.9%, 15%, and 15.4% using device architectures ranging from titania sensitized with active layer to mesosuperstructure, inert scaffold, and planar p–n junction.

$CH_3NH_3PbI_{3-x}Cl_x$ active layer by solution processing, it is difficult to form a uniform active layer of $CH_3NH_3PbI_3$ by solution processing. Schematics of device architecture are sketched in Figure 3.

7. Hybrid Perovskite Solar Cells

P3HT/PCBM blend has been extensively explored in organic photovoltaic applications. P3HT was replaced with $CH_3NH_3PbI_3$ as photoactive layer in planar heterojunction solar cell achieving a PCE of 3.9% [59]. Better wettability was achieved with PEDOT : PSS coated ITO substrate with DMF solution rather than coating perovskite active layer with γ-butyrolactone solution. A device structure based on $TiO_2/CH_3NH_3PbI_{3-x}Cl_x$/P3HT achieved better photovoltaic performance when the ITO substrate was treated with C60 self-assembled monolayer. PCE was improved from 3.8 to 6.7% with the incorporation of self-assembled monolayer. This was achieved with a significant increase in both Jsc and Voc [60]. Concept of hybrid planar heterojunction cell incorporating 285 nm thick layer of $CH_3NH_3PbI_3$ was investigated recently. Active layer was sandwiched between hole-transporting poly(N,N′-bis(4-butylphenyl)-N,N′-bis(phenyl)-benzidine) (poly-TPD) layer (10 nm) and electron accepting PCBM layer (10 nm) resulting in a PCE of 12% [61]. Charge collecting layers were solution-processed in spin-coated chlorobenzene while the active layer was vacuum-deposited by heating of reagents CH_3NH_3I to 70°C and PbI_2 to 250°C.

8. Flexible Perovskite Solar Cells

Low temperature solution processability of perovskite solar cells makes it possible to fabricate cells on flexible substrates. Ability to conform to the contours of the platform holds obvious promises for incorporation of this technology in diverse applications. $CH_3NH_3PbI_{3-x}Cl_x$ as active layer with PEDOT : PSS and PCBM as hole-transporting and electron selective contacts, respectively, have been investigated in regular and inverted device architecture on an ITO coated PET substrate achieving a PCE of 6.4% [62]. A higher PCE of 10.2% was achieved using device structure of ITO/ZnO (25 nm)/$CH_3NH_3PbI_3$/spiro-MeOTAD/Ag, fabricated using low temperature solution processing techniques [63]. ITO coated PEN substrate has been used to demonstrate a wearable perovskite based energy source achieving a PCE of 12.2% with only 5% loss over 1000 bending cycles of radius 10 mm [64].

9. Hybrid Multijunction Solar Cells

With the current state of the art, perovskite solar cells can be used effectively as a top cell, in a tandem cell configuration [65], with existing technologies like crystalline silicone and thin film solar cells like CZTSSe, CIGS [66], and CIS. With a reasonable estimate of achieving 20 mA cm^{-2} and Voc of 1.1 V at the top perovskite cell, a silicon cell generating 0.75 V Voc [67] will lead to a FF of 0.8 and an efficiency of 29.6% [68]. This all is possible with the existing technologies at hand with little optimization in terms of band gap widening, FF enhancement, and integration into tandem cell architecture [69, 70].

10. Balanced Electron- and Hole-Transporting Properties

Determination of diffusion lengths of electrons and holes in an active layer is vital parameter which dictates the optimal device architecture. If the diffusion length of the charges is smaller than the absorption depth, a mesostructured device is suitable for obtaining optimal charge collection. On the contrary planar junction devices are suited for efficient charger

collection and transport, without significant recombination, for larger diffusion lengths.

Transient photoluminescence (PL) and transient absorption spectroscopy measurements were used by Xing et al. [71, 72], and Stranks et al. [73], to report transport properties of $CH_3NH_3PbI_3$ and $CH_3NH_3PbI_{3-x}Cl_x$. Diffusion lengths for electrons and holes were reported at 129 nm (130 nm) and ~105 nm (90 nm), respectively, in $CH_3NH_3PbI_3$ and at ~1069 nm and ~1213 nm, respectively, in $CH_3NH_3PbI_{3-x}Cl_x$ [71, 73]. Thus it is evident that optimal architecture for $CH_3NH_3PbI_3$ is mesostructured cell while for $CH_3NH_3PbI_{3-x}Cl_x$, planar geometry will yield the highest PCE. Comparable decay time of photoinduced absorption at ~550 nm in transient absorption spectroscopy and transient PL has indirectly confirmed the generation of weakly bound photogenerated excitons in $CH_3NH_3PbI_{3-x}Cl_x$. Data from dielectric constant, transient absorption spectroscopy, impedance spectroscopy, and transient photoluminescence for perovskite materials suggest that the excitons generated are Wannier-type [74].

11. Band Gap Engineering of Perovskite Materials

Semiconductors with a band gap of 1.1 V are considered most suitable for harvesting the solar spectrum from visible to NIR. Strength of the potential developed is dependent on this band gap, with low potential leading to drawing of extra current at the expense of reduced voltage. The balancing of these two parameters dictates the optimal band gap in the range of 1.4 eV for cells made of single material [75]. Research has indicated that band gap in perovskites decreases with increase in dimensionality of $MO(X)_6$ network [76], increase in the angle of M–O(X)–M bonds [77], decrease in electronegativity of anions [78–82], and decrease in difference of electronegativity between metal cation and anion. Perovskite structure incorporating mixed iodide and bromide [31, 49, 83] or bromide and chloride [84] halide has continuously tuneable band gap allowing for light harvesting over the complete solar spectrum. Mixed chloride iodide halide perovskite renders no obvious band gap tuning owing to difficulty in incorporating Cl^- ion into PbI_6 octahedron [33, 85]. Energy levels of typical absorbers, hole selective contacts, and electron selective contacts are illustrated in Figure 4.

12. Improving Fill Factor

Low conductivity of HTM is the major reason for low FF of perovskite solar cells which can be remedied by doping the HTM with p-type codopant. Lithium salt Li-TFSI added to spiro-MeOTAD increases the hole conductivity in spiro-MeOTAD [86]. Photoelectron spectroscopy combined with absorbance measurements revealed that the Fermi level in spiro-MeOTAD is shifted toward HOMO due to the oxidation of 24% spiro-MeOTAD molecules by the addition of Li-TFSI [87]. Cobalt complexes based p-dopants in spiro-MeOTAD have been used to enhance the fill factor in ss DSSC [88]. p-dopant coded FK209 (tris (2-(1H-pyrazol-1-yl)-4-tert-butylpyridine)-cobalt(III)-tris (bis(trifuoromethylsulfonyl)imide)) to the spiro-MeOTAD, together with Li-TFSI and tBP, has been used to enhance the photovoltaic properties of $CH_3NH_3PbI_3$ activated solar cells by increasing the FF and Voc [89]. Protic ionic liquid has also been used recently as p-dopant to HTMs [90]. In addition to use of doping technique to improve the FF, improving the morphology (defect- and pinhole-free) of the active layer enhances the FF by enhancing the conductivity of HTM and reducing the series resistance. Establishing perfect p–n contact between active layer and HTM also improves the fill factor. Chemical modification can be used to fine-tune this contact between organic and inorganic layers from HTM and perovskite, respectively.

13. Fabrication Techniques

Approaches reported for the synthesis of perovskite active layers are one-step precursor solution deposition [72]; two-step sequential deposition [91]; dual-source vapor deposition [59]; vapor assisted solution process [92]; and sequential vapor deposition [93]. $CH_3NH_3PbX_3$ perovskites have been reported with both one-step and two-step coating techniques. Im et al. [43] first reported the one-step coating method for iodide perovskite active layer by reacting equimolar CH_3NH_2 and HI in the appropriate solvent. The white precipitates were obtained by introducing ethyl ether to the resulting solution, followed by vacuum drying for about 12 h. The synthesized CH_3NH_3I was then mixed with PbI_2 at a 1 : 1 molar ratio in γ-butyrolactone at 60°C and used as a coating solution. For two-step coating method lead iodide film is first formed on titania surface through spin coating or vacuum deposition and the layer thus formed is immersed in CH_3NH_3I [91, 94] containing solution.

One-step solution processing is the simplest of the solution processing technique for the growth of perovskite layer. A precursor solution is spun-cast on substrate resulting in loss of excess solution, drying of solvent, and annealing of the solvent. While these processes proceed simultaneously, properties of the solvent, additives, and the annealing and processing temperatures and environments have a profound impact on the final film quality.

Solvents reported for optimum solution process are typically γ-butyrolactone (GBL), dimethylformamide (DMF), and dimethyl sulfoxide (DMSO). GBL gives a lower maximum concentration of solute at 40 wt% [43] while DMF and DMSO give higher loading of 60 wt% at room temperatures [95]. Mixture of solvents has also been reported for obtaining optimum concentrations for solution processing since higher concentrations lead to better film coverage and higher efficiency devices [72, 73, 96]. Best results are reported for a combination of DMF and GBL (3 : 97 vol%) owing to the rapid evaporation of this combination of solvents [74, 97]. Application of solvents like toluene during spin coating at the surface of the perovskite film leads to better concentration and uniform morphology. This is attributed to the rinsing of excess solvent by toluene leading to better crystallization of perovskites [98].

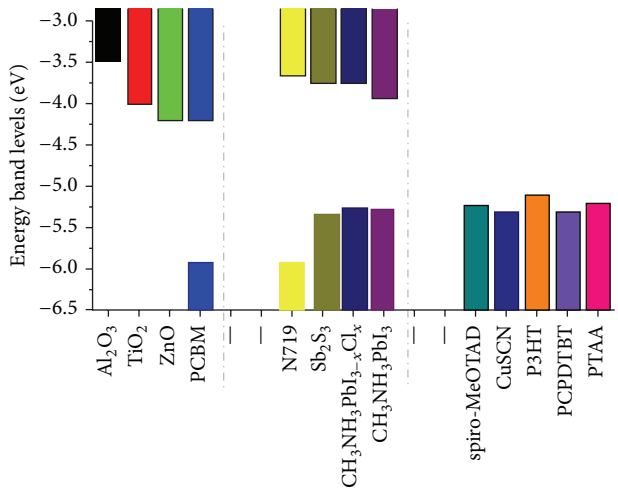

Figure 4: Energy level illustration for different ETM (left), absorbers (center), and HTM (right) in solar cells.

Perovskite film coverage is also dependent upon annealing temperature during solution processing by one-step solution method [99]. Lower annealing temperature results in poor film convergence while higher annealing temperatures lead to decomposition of active layer [100]. Optimum annealing conditions are reported to be slow annealing at 100°C forming particles of 100–1000 nm [101].

Improvement in film formation was made possible by two-step sequential deposition [91, 94], within the realm of solution processing. Two-step methods afford higher loading of lead iodide by first spin casting of lead iodide followed by solution processing or vacuum assisted deposition of MAI [93]. It is a heterophase reaction resulting in conversion to $MAPbI_3$. This results in a more compact, uniform, and reproducible film. Alterations have been adopted by different researchers to optimize this process, including prewetting [102] the lead iodide film in dispersion solvent and heating the substrate resulting in higher efficiencies [91, 102, 103]. Successive spin coating method, an improvement over two-step method, has also been used to improve the film formation [104]. Use of DMSO, a strong coordinated solvent, for solution processing of PbI_2 results in amorphous film ensuring smooth and uniform coverage and complete conversion to $MAPbI_3$ [105].

A modification of two-step deposition method is the vapor assisted growth of MAI on the PbI_2 film. Compact and uniform PbI_2 film obtained by solution processing is exposed to MAI vapors under ambient conditions. In contrast to vapor deposition this method does not require expensive vacuum equipment and environmental controls. Combining the advantages of solution processing and low temperature vapor deposition, the films grown are pinhole-free offering higher efficiencies [93, 106]. Doctor blade [107], liquid droplet assisted two-step solution process [108], spray and brush solution processing [109], and flash evaporation [110] have also been recently reported to add to the versatility of synthesis techniques.

14. Stability Studies

Two parameters important for commercial application of perovskite solar cells are stability and efficiency. Lots of research effort has been directed at enhancing the efficiency of these devices by adoption of various device architectures, compositions, and manufacturing techniques. This has resulted in substantial increase in efficiencies to a proven efficiency of 20.1 [111]. The limiting factor to this success story is the efficiency. High efficiency devices reported are synthesized under controlled environments and lose their efficiencies rapidly. For their commercial viability it is imperative that studies be undertaken on issues of stability and reproducibility to enhance the lifetime of these devices. Degradation in perovskite solar cells is a synergetic effect of exposure to humidity, oxygen, ultraviolet radiations, and temperatures.

Niu et al. have proposed a sequence of chemical reactions considered responsible for the degradation of $CH_3NH_3PbI_3$ in the presence of moisture [16]:

$$CH_3NH_3PbI_3\,(s) \longleftrightarrow PbI_2\,(s) + CH_3NH_3I\,(aq) \quad (1)$$

$$CH_3NH_3I\,(aq) \longleftrightarrow CH_3NH_2\,(aq) + HI\,(aq) \quad (2)$$

$$4HI\,(aq) + O_2\,(g) \longleftrightarrow 2I_2\,(s) + 2H_2O\,(l) \quad (3)$$

$$2HI\,(aq) \longleftrightarrow H_2\,(g) + I_2\,(s) \quad (4)$$

The equilibrium species, in the presence of water, oxygen, and UV radiation, are thus CH_3NH_3I, CH_3NH_2, and HI. HI can either decompose by a one-step redox reaction (3) or by photochemical reaction under UV radiation to H_2 and I_2. This sensitivity requires synthesis in a controlled environment like a glove box [59, 91]. A humidity of 55% is reported to deteriorate performance and is evident by a color change from dark brown to yellow [49]. Devices incorporating Al_2O_3 scaffold showed better stability in line with the reports on stability of DSSC with this scaffold [112,

113]. $CH_3NH_3PbBr_3$ is reported to be more stable to moisture exposure and $CH_3NH_3Pb(I_{1-x}Br_x)_3$ based absorbers retained good PCE on exposure to humidity of 55% for 20 days [49]. A moisture induced reconstruction mechanism has also been proposed for controlled humidity synthesis in planar geometry. Though the efficiency increased to 19.3%, it rapidly deteriorated to less than 5% of original performance when stored in ambient conditions [110]. Encapsulation techniques developed for CIGS based devices could prove effective in addressing the moisture sensitivity of these devices [114]. A PCE of 15.76% has been achieved for devices synthesized in ambient conditions with humidity of 50% by incorporating a substrate preheating step before spin-coating lead iodide [115].

UV sensitivity is attributed to use of TiO_2 as photoanode in PSC. With a band gap of 3.2 eV, it is typically a photocatalyst for oxidizing water and organic matter [116]. Proposed degradation mechanism for $CH_3NH_3PbI_3$ under UV illumination is [117]

$$2I^- \longleftrightarrow I_2 + 2e^- \quad \left[\text{at the interface between } TiO_2 \text{ and } CH_3NH_3PbI_3\right] \tag{5a}$$

$$3CH_3NH_3{}^+ \longleftrightarrow 3CH_3NH_2 \uparrow + 3H^+ \tag{5b}$$

$$I^- + I_2 + 3H^+ + 2e^- \longleftrightarrow 3HI \uparrow \tag{5c}$$

Inclusion of Sb_2S_3 layer at the interface between mesoporous TiO_2 and perovskite layer was observed to increase the stability, attributed to the interruption of iodide couple at the interface. UV activated decay at the interface of TiO_2 is also reported to be arrested by the presence of oxygen which removes surface states and pacifies deep trap sites at the interface, titania being an n-type semiconductor [118, 119]. Use of alumino silicate shell on titania nanoparticles can increase stability [119]. Al_2O_3 scaffold is a more stable alternate to TiO_2 in MSSC [118, 120].

Thermal stability studies are important as under solar illumination the temperatures are expected to be over the phase transition temperature of $CH_3NH_3PbI_3$. It changes from tetragonal to cubic structure at 56°C [121]. Studies have indicated that thermal stability can be affected by subtle variations in synthesis routes and the precursors used [122]. Poor thermal conductivity by monocrystalline and polycrystalline $CH_3NH_3PbI_3$ also creates internal stresses to the detriment of the mechanical integrity of the films and hence the lifetime of the devices [123]. Use of polymers with single-walled CNTs as a HTL has been reported to increase the thermal stability and retard moisture sensitivity of the perovskite solar cells [124]. Issue of lead poisoning has been simulated by investigating the effect of rain with water of different pH values concluding that the use is environmentally safe [125].

15. Hysteresis Effects

Ferroelectric polarization of perovskites has been under focus recently. Understanding the ferroelectric behaviour of this class of materials may be critical in increasing its efficiency and stability as ferroelectricity may affect the photoexcited electron hole pairing and separation [126, 127]. The origins of this effect are still postulated. Ferroelectricity came under focus on the reports of hysteresis behaviour in current voltage scans [128–130], dependent on the scan rate and direction [129], light soaking history [128], and contact material and interfaces [131]. Snaith et al. have proposed capacitive effects, ferroelectric behavior of absorber, and defect densities to be the source of hysteresis behaviour [131]. This effect, if not accounted for, results in erroneous efficiency values in comparison to the stabilized output [132]. Conflicting reports through theoretical and experimental values have added impetus to the current research. The observed hysteresis in current voltage (JV) curves was attributed to ferroelectric domain under applied electric field, while the same effect can also be caused by ionic migration [131, 133] or trapping detrapping [131, 134] of charge carriers. Identification of polar I4 cm space group [135] instead of previously accepted nonpolar I4/mcm [131, 133] had added weight to the theory of ferroelectric polarization. Theoretical calculations have postulated a polarization value of 38 $\mu C/cm^2$ [126].

Studies of polarization electric field [130] were used to investigate the ferroelectric response of $CH_3NH_3PbI_3$, though they were heavily distorted by leakage currents and may not be conclusive evidence to the ferroelectric response. Piezoresponse force microscopy [136] indicated ferroelectric domains though no confirmation of local switching of ferroelectric domains was presented. Concurrent evaluation of PE loops and piezoresponse force microscopy by Xiao et al. [137] in a recent report did not detect ferroelectric polarization in contrast to the other reports. Many reports have supported a ferroelectric response [129, 130, 135, 136, 138] by this class of materials. Understanding the physical phenomenon responsible for this effect is vital for efficiency enhancement and is an open area of research. Physical optimization by trial and error and theoretical simulations will lead to stabilized efficiencies and will add to maturing of this technology.

16. Comparison to Other Technologies

Solar cell has to absorb sun light and convert its incident energy into electrical power. The energy of incident photons is scattered over the entire spectrum of solar radiations. Photons with energy equal to the band gap of the active layer in a PV cell only are absorbed while photons with energy lower than the band gap are not absorbed at all while photons with energy higher than the band gap generate electron above the conduction band which lose their energy in the form of heat, while relaxing back to valence band. Thus the maximum voltage solar cells generate is the open circuit voltage and it indicates the maximum electrical power derivable form the incident photons.

Perovskites are unique as active layer in PV modules owing to their ability to deliver high open circuit voltages, under full sun illumination, leading to light harvesting from a broad spectrum of incident solar radiation. Voc is a measure of the maximum energy that can be drawn from the incident photon by the solar cell. The difference between Voc and the potential of the lowest energy photon generating a charge is a measure of the fundamental loss in a solar

cell [139]. Thermodynamic treatment limits this loss to the tune of 250–300 meV, varying with the band gap, based on Shockley-Queisser treatment [75]. Onset of the IPCE spectrum determines the lowest energy absorbed photon. For $CH_3NH_3I_{3-x}Cl_x$ perovskite the onset is 1.55 eV (800 nm) and the best Voc of 1.1 gives a loss in potential of 450 meV which is lower than the reported loss of 0.59 eV for best commercially available PV technology CdTe at an efficiency of 19.6% [140]. Thus perovskite solar cells, at the current state of the art, are at par with commercial technologies like CIGS, GaAs, and crystalline silicon [141].

17. Future Outlook

In a span of a couple of years, perovskites have demonstrated that they possess the right mix of properties to offer a solution to our energy requirements. Though they evolved out of liquid electrolyte DSSCs, they are now established as a class of their own with extensive research focus pushing the efficiency limit beyond 20%. Low temperature solution processing assures low per watt cost and quick energy payback times. Device architectures ranging from pin [55, 59, 99] to mesoporous to mesosuperstructure configuration throw wide open the possibilities for incorporation of novel materials and synthesis approaches. The future may hold no scaffold pin planar configuration or the incorporation of other semiconductor materials for inert oxide scaffold. Use of materials with high mobility as HTM will further improve the FF while optimization of the interfaces and selection of HTM and ETM may push forward the efficiencies to higher values. Incorporation of narrow band gap perovskites and plasmonic light harvester may broaden the spectral response with better light harvesting. Interface engineering and introduction of self-assembled layers will reduce losses and improve efficiency. Understanding of the underlying photophysical phenomenon will further help improving device structures and better selection of materials. Exploration of tandem cell configuration with perovskite based cell as the top cell will push forward the achievable efficacy limit further. With the amount of research effort under way, guided by the adherence to the issue of best practices [142], this technology holds great promise to addressing our energy concerns. Addressing the issues of stability and use of lead can go a long way in maturing this technology for commercial application, though in the present legal framework use of lead is not a problem as CdTe based solar cell has received wide acceptance despite Cd content. Use of lead extensively in lead acid batteries and its content at comparable levels in CIGS and silicon modules to perovskites [143] suggest that in the short term the concern may not be pressing, but these technologies are increasingly being phased out and alternatives are explored to minimize the environmental impacts of these heavy metals. Replacement of lead with tin in perovskite solar cell is already under investigation and may offer an environment friendly alternative [144].

Conflict of Interests

The authors declare that there is no conflict of interests regarding the publication of this paper.

References

[1] M. A. Green, K. Emery, Y. Hishikawa, W. Warta, and E. D. Dunlop, "Solar cell efficiency tables (version 40)," *Progress in Photovoltaics: Research and Applications*, vol. 20, no. 5, pp. 606–614, 2012.

[2] M. A. Green, "Silicon solar cells: evolution, high-efficiency design and efficiency enhancements," *Semiconductor Science and Technology*, vol. 8, no. 1, pp. 1–12, 1993.

[3] J. Britt and C. Ferekides, "Thin-film CdS/CdTe solar cell with 15.8% efficiency," *Applied Physics Letters*, vol. 62, no. 22, article 2851, 1993.

[4] I. Repins, M. A. Contreras, B. Egaas et al., "19.9%-efficient ZnO/CdS/CuInGaSe^2 solar cell with 81.2% fill factor," *Progress in Photovoltaics: Research and Applications*, vol. 16, no. 3, pp. 235–239, 2008.

[5] M. Graetzel, R. A. J. Janssen, D. B. Mitzi, and E. H. Sargent, "Materials interface engineering for solution-processed photovoltaics," *Nature*, vol. 488, no. 7411, pp. 304–312, 2012.

[6] J. J. M. Halls, C. A. Walsh, N. C. Greenham et al., "Efficient photodiodes from interpenetrating polymer networks," *Nature*, vol. 376, no. 6540, pp. 498–500, 1995.

[7] B. O'Regan and M. Grätzel, "A low-cost, high-efficiency solar cell based on dye-sensitized colloidal TiO_2 films," *Nature*, vol. 353, no. 6346, pp. 737–740, 1991.

[8] C. W. Tang, "Two-layer organic photovoltaic cell," *Applied Physics Letters*, vol. 48, no. 2, article 183, 1986.

[9] T. K. Todorov, K. B. Reuter, and D. B. Mitzi, "High-efficiency solar cell with earth-abundant liquid-processed absorber," *Advanced Materials*, vol. 22, no. 20, pp. E156–E159, 2010.

[10] G. Li, V. Shrotriya, J. Huang et al., "High-efficiency solution processable polymer photovoltaic cells by self-organization of polymer blends," *Nature Materials*, vol. 4, no. 11, pp. 864–868, 2005.

[11] M. A. Green, A. Ho-Baillie, and H. J. Snaith, "The emergence of perovskite solar cells," *Nature Photonics*, vol. 8, no. 7, pp. 506–514, 2014.

[12] G. Hodes and D. Cahen, "Photovoltaics: perovskite cells roll forward," *Nature Photonics*, vol. 8, no. 2, pp. 87–88, 2014.

[13] S. H. Im, J.-H. Heo, H. J. Han, D. Kim, and T. Ahn, "18.1% hysteresis-less inverted $CH_3NH_3PbI_3$ planar perovskite hybrid solar cells," *Energy & Environmental Science*, vol. 8, pp. 1602–1608, 2015.

[14] J. H. Heo, D. H. Song, H. J. Han et al., "Planar $CH_3NH_3PbI_3$ perovskite solar cells with constant 17.2% average power conversion efficiency irrespective of the scan rate," *Advanced Materials*, 2015.

[15] P. P. Boix, K. Nonomura, N. Mathews, and S. G. Mhaisalkar, "Current progress and future perspectives for organic/inorganic perovskite solar cells," *Materials Today*, vol. 17, no. 1, pp. 16–23, 2014.

[16] G. Niu, X. Guo, and L. Wang, "Review of recent progress in chemical stability of perovskite solar cells," *Journal of Materials Chemistry A*, vol. 3, pp. 8970–8980, 2014.

[17] S. Luo and W. A. Daoud, "Recent progress in organic-inorganic halide perovskite solar cells: mechanisms and materials design," *Journal of Materials Chemistry A*, vol. 3, pp. 8992–9010, 2014.

[18] A. Kojima, K. Teshima, Y. Shirai, and T. Miyasaka, "Organometal halide perovskites as visible-light sensitizers for photovoltaic cells," *Journal of the American Chemical Society*, vol. 131, no. 17, pp. 6050–6051, 2009.

[19] R. F. Service, "Energy technology: perovskite solar cells keep on surging," *Science*, vol. 344, no. 6183, article 458, 2014.

[20] J. G. Bednorz and K. A. Muller, "Possible highT_c superconductivity in the Ba–La–Cu–O system," *Zeitschrift für Physik B Condensed Matter*, vol. 64, pp. 189–193, 1986.

[21] X. Xu, C. Randorn, P. Efstathiou, and J. T. S. Irvine, "A red metallic oxide photocatalyst," *Nature Materials*, vol. 11, no. 7, pp. 595–598, 2012.

[22] Z. Cheng and J. Lin, "Layered organic-inorganic hybrid perovskites: structure, optical properties, film preparation, patterning and templating engineering," *CrystEngComm*, vol. 12, no. 10, pp. 2646–2662, 2010.

[23] D. B. Mitzi, S. Wang, C. A. Feild, C. A. Chess, and A. M. Guloy, "Conducting layered organic-inorganic halides containing <110>-oriented perovskite sheets," *Science*, vol. 267, no. 5203, pp. 1473–1476, 1995.

[24] C. Li, X. Lu, W. Ding, L. Feng, Y. Gao, and Z. Guo, "Formability of ABX_3 (X = F, Cl, Br, I) halide perovskites," *Acta Crystallographica B*, vol. 64, pp. 702–707, 2008.

[25] B. N. Cohen, C. Labarca, N. Davidson, and H. A. Lester, "Mutations in M2 alter the selectivity of the mouse nicotinic acetylcholine receptor for organic and alkali metal cations," *Journal of General Physiology*, vol. 100, no. 3, pp. 373–400, 1992.

[26] J.-H. Im, J. Chung, S.-J. Kim, and N.-G. Park, "Synthesis, structure, and photovoltaic property of a nanocrystalline 2H perovskite-type novel sensitizer ($CH_3CH_2NH_3$)PbI_3," *Nanoscale Research Letters*, vol. 7, article 353, 2012.

[27] R. S. Sanchez, V. Gonzalez-Pedro, J.-W. Lee et al., "Slow dynamic processes in lead halide perovskite solar cells. Characteristic times and hysteresis," *Journal of Physical Chemistry Letters*, vol. 5, no. 13, pp. 2357–2363, 2014.

[28] N. K. McKinnon, D. C. Reeves, and M. H. Akabas, "5-HT3 receptor ion size selectivity is a property of the transmembrane channel, not the cytoplasmic vestibule portals," *Journal of General Physiology*, vol. 138, no. 4, pp. 453–466, 2011.

[29] S. Pang, H. Hu, J. Zhang et al., "$NH_2CH{=}NH_2PbI_3$: an alternative organolead iodide Perovskite sensitizer for mesoscopic solar cells," *Chemistry of Materials*, vol. 26, no. 3, pp. 1485–1491, 2014.

[30] S. Lv, S. Pang, Y. Zhou et al., "One-step, solution-processed formamidinium lead trihalide ($FAPbI_{(3-x)}CI_x$) for mesoscopic perovskite-polymer solar cells," *Physical Chemistry Chemical Physics*, vol. 16, no. 36, pp. 19206–19211, 2014.

[31] G. E. Eperon, S. D. Stranks, C. Menelaou, M. B. Johnston, L. M. Herz, and H. J. Snaith, "Formamidinium lead trihalide: a broadly tunable perovskite for efficient planar heterojunction solar cells," *Energy and Environmental Science*, vol. 7, no. 3, pp. 982–988, 2014.

[32] P. Umari, E. Mosconi, and F. De Angelis, "Relativistic GW calculations on $CH_3NH_3PbI_3$ and $CH_3NH_3SnI_3$ perovskites for solar cell applications," *Scientific Reports*, vol. 4, article 4467, 2014.

[33] M. M. Lee, J. Teuscher, T. Miyasaka, T. N. Murakami, and H. J. Snaith, "Efficient hybrid solar cells based on meso-superstructured organometal halide perovskites," *Science*, vol. 338, no. 6107, pp. 643–647, 2012.

[34] H. J. Snaith and L. Schmidt-Mende, "Advances in liquid-electrolyte and solid-state dye-sensitized solar cells," *Advanced Materials*, vol. 19, no. 20, pp. 3187–3200, 2007.

[35] H. J. Snaith, A. Stavrinadis, P. Docampo, and A. A. R. Watt, "Lead-sulphide quantum-dot sensitization of tin oxide based hybrid solar cells," *Solar Energy*, vol. 85, no. 6, pp. 1283–1290, 2011.

[36] H. Lee, H. C. Leventis, S.-J. Moon et al., "PbS and CdS quantum dot-sensitized solid-state solar cells: 'old concepts, new results'," *Advanced Functional Materials*, vol. 19, no. 17, pp. 2735–2742, 2009.

[37] P. V. Kamat, "Quantum dot solar cells. Semiconductor nanocrystals as light harvesters," *Journal of Physical Chemistry C*, vol. 112, no. 48, pp. 18737–18753, 2008.

[38] Y. Itzhaik, O. Niitsoo, M. Page, and G. Hodes, "Sb_2S_3-sensitized nanoporous TiO_2 solar cells," *The Journal of Physical Chemistry C*, vol. 113, no. 11, pp. 4254–4256, 2009.

[39] P. V. Kamat, "Quantum dot solar cells. The next big thing in photovoltaics," *Journal of Physical Chemistry Letters*, vol. 4, no. 6, pp. 908–918, 2013.

[40] A. Kojima, K. Teshima, T. Miyasaka, and Y. Shirai, "Novel photoelectrochemical cell with mesoscopic electrodes sensitized by lead-halide compounds (2)," *ECS Meeting Abstracts*, absrtact MA2006-02, p. 397, 2006.

[41] H.-S. Kim, C.-R. Lee, J.-H. Im et al., "Lead iodide perovskite sensitized all-solid-state submicron thin film mesoscopic solar cell with efficiency exceeding 9%," *Scientific Reports*, vol. 2, article 591, 2012.

[42] A. Kojima, K. Teshima, Y. Shirai, and T. Miyasaka, "Novel photoelectrochemical cell with mesoscopic electrodes sensitized by lead-halide compounds (11)," *ECS Meeting*, vol. 27, abstract MA2008-02, 2008.

[43] J.-H. Im, C.-R. Lee, J.-W. Lee, S.-W. Park, and N.-G. Park, "6.5% efficient perovskite quantum-dot-sensitized solar cell," *Nanoscale*, vol. 3, no. 10, pp. 4088–4093, 2011.

[44] B. E. Hardin, H. J. Snaith, and M. D. McGehee, "The renaissance of dye-sensitized solar cells," *Nature Photonics*, vol. 6, no. 3, pp. 162–169, 2012.

[45] U. Bach, D. Lupo, P. Comte et al., "Solid-state dye-sensitized mesoporous TiO_2 solar cells with high photon-to-electron conversion efficiencies," *Nature*, vol. 395, no. 6702, pp. 583–585, 1998.

[46] J. Burschka, A. Dualeh, F. Kessler et al., "Tris(2-(1*H*-pyrazol-1-yl)pyridine)cobalt(III) as p-type dopant for organic semiconductors and its application in highly efficient solid-state dye-sensitized solar cells," *Journal of the American Chemical Society*, vol. 133, no. 45, pp. 18042–18045, 2011.

[47] L. Etgar, P. Gao, Z. Xue et al., "Mesoscopic $CH_3NH_3PbI_3/TiO_2$ heterojunction solar cells," *Journal of the American Chemical Society*, vol. 134, no. 42, pp. 17396–17399, 2012.

[48] W. A. Laban and L. Etgar, "Depleted hole conductor-free lead halide iodide heterojunction solar cells," *Energy and Environmental Science*, vol. 6, no. 11, pp. 3249–3253, 2013.

[49] J. H. Noh, S. H. Im, J. H. Heo, T. N. Mandal, and S. I. Seok, "Chemical management for colorful, efficient, and stable inorganic-organic hybrid nanostructured solar cells," *Nano Letters*, vol. 13, no. 4, pp. 1764–1769, 2013.

[50] H.-S. Kim, J.-W. Lee, N. Yantara et al., "High efficiency solid-state sensitized solar cell-based on submicrometer rutile TiO_2 nanorod and $CH_3NH_3PbI_3$ perovskite sensitizer," *Nano Letters*, vol. 13, no. 6, pp. 2412–2417, 2013.

[51] E. Edri, S. Kirmayer, D. Cahen, and G. Hodes, "High open-circuit voltage solar cells based on organic-inorganic lead bromide perovskite," *The Journal of Physical Chemistry Letters*, vol. 4, no. 6, pp. 897–902, 2013.

[52] J. Qiu, Y. Qiu, K. Yan et al., "All-solid-state hybrid solar cells based on a new organometal halide perovskite sensitizer and one-dimensional TiO_2 nanowire arrays," *Nanoscale*, vol. 5, no. 8, pp. 3245–3248, 2013.

[53] B. Cai, Y. Xing, Z. Yang, W.-H. Zhang, and J. Qiu, "High performance hybrid solar cells sensitized by organolead halide perovskites," *Energy and Environmental Science*, vol. 6, no. 6, pp. 1480–1485, 2013.

[54] D. Bi, L. Yang, G. Boschloo, A. Hagfeldt, and E. M. J. Johansson, "Effect of different hole transport materials on recombination in $CH_3NH_3PbI_3$ perovskite-sensitized mesoscopic solar cells," *Journal of Physical Chemistry Letters*, vol. 4, no. 9, pp. 1532–1536, 2013.

[55] J. M. Ball, M. M. Lee, A. Hey, and H. J. Snaith, "Low-temperature processed meso-superstructured to thin-film perovskite solar cells," *Energy and Environmental Science*, vol. 6, no. 6, pp. 1739–1743, 2013.

[56] M. J. Carnie, C. Charbonneau, M. L. Davies et al., "A one-step low temperature processing route for organolead halide perovskite solar cells," *Chemical Communications*, vol. 49, no. 72, pp. 7893–7895, 2013.

[57] H.-S. Kim, I. Mora-Sero, V. Gonzalez-Pedro et al., "Mechanism of carrier accumulation in perovskite thin-absorber solar cells," *Nature Communications*, vol. 4, article 2242, 2013.

[58] D. Bi, S.-J. Moon, L. Häggman et al., "Using a two-step deposition technique to prepare perovskite ($CH_3NH_3PbI_3$) for thin film solar cells based on ZrO_2 and TiO_2 mesostructures," *RSC Advances*, vol. 3, no. 41, pp. 18762–18766, 2013.

[59] M. Liu, M. B. Johnston, and H. J. Snaith, "Efficient planar heterojunction perovskite solar cells by vapour deposition," *Nature*, vol. 501, no. 7467, pp. 395–398, 2013.

[60] J.-Y. Jeng, Y.-F. Chiang, M.-H. Lee et al., "$CH_3NH_3PbI_3$ perovskite/fullerene planar-heterojunction hybrid solar cells," *Advanced Materials*, vol. 25, no. 27, pp. 3727–3732, 2013.

[61] A. Abrusci, S. D. Stranks, P. Docampo, H.-L. Yip, A. K.-Y. Jen, and H. J. Snaith, "High-performance perovskite-polymer hybrid solar cells via electronic coupling with fullerene monolayers," *Nano Letters*, vol. 13, no. 7, pp. 3124–3128, 2013.

[62] O. Malinkiewicz, A. Yella, Y. H. Lee et al., "Perovskite solar cells employing organic charge-transport layers," *Nature Photonics*, vol. 8, no. 2, pp. 128–132, 2014.

[63] P. Docampo, J. M. Ball, M. Darwich, G. E. Eperon, and H. J. Snaith, "Efficient organometal trihalide perovskite planar-heterojunction solar cells on flexible polymer substrates," *Nature Communications*, vol. 4, article 2761, 2013.

[64] B. J. Kim, D. H. Kim, Y. Lee et al., "Highly efficient and bending durable perovskite solar cells: toward a wearable power source," *Energy & Environmental Science*, vol. 8, no. 3, pp. 916–921, 2015.

[65] Z. M. Beiley and M. D. McGehee, "Modeling low cost hybrid tandem photovoltaics with the potential for efficiencies exceeding 20%," *Energy and Environmental Science*, vol. 5, no. 11, pp. 9173–9179, 2012.

[66] C. D. Bailie, M. G. Christoforo, J. P. Mailoa et al., "Polycrystalline tandem photovoltaics using perovskites on top of silicon and CIGS," *Energy & Environmental Science*, vol. 8, pp. 956–963, 2014.

[67] K. D. Karlin, Ed., *Progress in Inorganic Chemistry*, vol. 48, John Wiley & Sons, New York, NY, USA, 1999.

[68] H. J. Snaith, "Perovskites: the emergence of a new era for low-cost, high-efficiency solar cells," *Journal of Physical Chemistry Letters*, vol. 4, no. 21, pp. 3623–3630, 2013.

[69] J. P. Mailoa, C. D. Bailie, E. C. Johlin et al., "A 2-terminal perovskite/silicon multijunction solar cell enabled by a silicon tunnel junction," *Applied Physics Letters*, vol. 106, no. 12, Article ID 121105, 2015.

[70] H. Uzu, M. Ichikawa, M. Hino et al., "High efficiency solar cells combining a perovskite and a silicon heterojunction solar cells via an optical splitting system," *Applied Physics Letters*, vol. 106, no. 1, Article ID 013506, 2015.

[71] D. Liu and T. L. Kelly, "Perovskite solar cells with a planar heterojunction structure prepared using room-temperature solution processing techniques," *Nature Photonics*, vol. 8, no. 2, pp. 133–138, 2014.

[72] G. Xing, N. Mathews, S. Sun et al., "Long-range balanced electron-and hole-transport lengths in organic-inorganic $CH_3NH_3PbI_3$," *Science*, vol. 342, no. 6156, pp. 344–347, 2013.

[73] S. D. Stranks, G. E. Eperon, G. Grancini et al., "Electron-hole diffusion lengths exceeding 1 micrometer in an organometal trihalide perovskite absorber," *Science*, vol. 342, no. 6156, pp. 341–344, 2013.

[74] H.-S. Kim, S. H. Im, and N.-G. Park, "Organolead halide perovskite: new horizons in solar cell research," *Journal of Physical Chemistry C*, vol. 118, no. 11, pp. 5615–5625, 2014.

[75] W. Shockley and H. J. Queisser, "Detailed balance limit of efficiency of p–n junction solar cells," *Journal of Applied Physics*, vol. 32, no. 3, pp. 510–519, 1961.

[76] Y. Takeoka, K. Asai, M. Rikukawa, and K. Sanui, "Systematic studies on chain lengths, halide species, and well thicknesses for lead halide layered perovskite thin films," *Bulletin of the Chemical Society of Japan*, vol. 79, no. 10, pp. 1607–1613, 2006.

[77] J. L. Knutson, J. D. Martin, and D. B. Mitzi, "Tuning the band gap in hybrid tin iodide perovskite semiconductors using structural templating," *Inorganic Chemistry*, vol. 44, no. 13, pp. 4699–4705, 2005.

[78] H. W. Eng, P. W. Barnes, B. M. Auer, and P. M. Woodward, "Investigations of the electronic structure of d0 transition metal oxides belonging to the perovskite family," *Journal of Solid State Chemistry*, vol. 175, no. 1, pp. 94–109, 2003.

[79] J. Etourneau, J. Portier, and F. Ménil, "The role of the inductive effect in solid state chemistry: how the chemist can use it to modify both the structural and the physical properties of the materials," *Journal of Alloys and Compounds*, vol. 188, pp. 1–7, 1992.

[80] M. Jansen and H. P. Letschert, "Inorganic yellow-red pigments without toxic metals," *Nature*, vol. 404, no. 6781, pp. 980–982, 2000.

[81] E. Knittle and R. Jeanloz, "Synthesis and equation of state of (Mg,Fe) SiO_3 perovskite to over 100 gigapascals," *Science*, vol. 235, no. 4789, pp. 668–670, 1987.

[82] R. Marchand, F. Tessier, A. Le Sauze, and N. Diot, "Typical features of nitrogen in nitride-type compounds," *International Journal of Inorganic Materials*, vol. 3, no. 8, pp. 1143–1146, 2001.

[83] S. A. Kulkarni, T. Baikie, P. P. Boix, N. Yantara, N. Mathews, and S. Mhaisalkar, "Band-gap tuning of lead halide perovskites using a sequential deposition process," *Journal of Materials Chemistry A*, vol. 2, no. 24, pp. 9221–9225, 2014.

[84] N. Kitazawa, Y. Watanabe, and Y. Nakamura, "Optical properties of $CH_3NH_3PbX_3$ (X = halogen) and their mixed-halide crystals," *Journal of Materials Science*, vol. 37, no. 17, pp. 3585–3587, 2002.

[85] S. Colella, E. Mosconi, P. Fedeli et al., "$MAPbI_{3-x}CI_x$ mixed halide perovskite for hybrid solar cells: the role of chloride as

dopant on the transport and structural properties," *Chemistry of Materials*, vol. 25, no. 22, pp. 4613–4618, 2013.

[86] H. J. Snaith and M. Grätzel, "Enhanced charge mobility in a molecular hole transporter via addition of redox inactive ionic dopant: Implication to dye-sensitized solar cells," *Applied Physics Letters*, vol. 89, no. 26, Article ID 262114, 2006.

[87] R. Schölin, M. H. Karlsson, S. K. Eriksson, H. Siegbahn, E. M. J. Johansson, and H. Rensmo, "Energy level shifts in spiro-OMeTAD molecular thin films when adding Li-TFSI," *Journal of Physical Chemistry C*, vol. 116, no. 50, pp. 26300–26305, 2012.

[88] J. Burschka, F. Kessler, M. K. Nazeeruddin, and M. Grätzel, "Co(III) complexes as p-dopants in solid-state dye-sensitized solar cells," *Chemistry of Materials*, vol. 25, no. 15, pp. 2986–2990, 2013.

[89] J. H. Noh, N. J. Jeon, Y. C. Choi, M. K. Nazeeruddin, M. Grätzel, and S. I. Seok, "Nanostructured $TiO_2/CH_3NH_3PbI_3$ heterojunction solar cells employing spiro-OMeTAD/Co-complex as hole-transporting material," *Journal of Materials Chemistry A*, vol. 1, no. 38, pp. 11842–11847, 2013.

[90] A. Abate, D. J. Hollman, J. Teuscher et al., "Protic ionic liquids as p-dopant for organic hole transporting materials and their application in high efficiency hybrid solar cells," *Journal of the American Chemical Society*, vol. 135, no. 36, pp. 13538–13548, 2013.

[91] J. Burschka, N. Pellet, S.-J. Moon et al., "Sequential deposition as a route to high-performance perovskite-sensitized solar cells," *Nature*, vol. 499, no. 7458, pp. 316–319, 2013.

[92] H. Zhou, Q. Chen, G. Li et al., "Interface engineering of highly efficient perovskite solar cells," *Science*, vol. 345, no. 6196, pp. 542–546, 2014.

[93] H. Hu, D. Wang, Y. Zhou et al., "Vapour-based processing of hole-conductor-free $CH_3NH_3PbI_3$ perovskite/C_{60} fullerene planar solar cells," *RSC Advances*, vol. 4, no. 55, pp. 28964–28967, 2014.

[94] K. Liang, D. B. Mitzi, and M. T. Prikas, "Synthesis and characterization of organic–inorganic perovskite thin films prepared using a versatile two-step dipping technique," *Chemistry of Materials*, vol. 10, no. 1, pp. 403–411, 1998.

[95] B. Conings, L. Baeten, C. De Dobbelaere, J. D'Haen, J. Manca, and H.-G. Boyen, "Perovskite-based hybrid solar cells exceeding 10% efficiency with high reproducibility using a thin film sandwich approach," *Advanced Materials*, vol. 26, no. 13, pp. 2041–2046, 2014.

[96] Y. Zhao, A. M. Nardes, and K. Zhu, "Solid-state mesostructured perovskite $CH_3NH_3PbI_3$ solar cells: charge transport, recombination, and diffusion length," *Journal of Physical Chemistry Letters*, vol. 5, no. 3, pp. 490–494, 2014.

[97] J. Seo, S. Park, Y. Chan Kim et al., "Benefits of very thin PCBM and LiF layers for solution-processed p–i–n perovskite solar cells," *Energy and Environmental Science*, vol. 7, no. 8, pp. 2642–2646, 2014.

[98] N. J. Jeon, J. H. Noh, Y. C. Kim, W. S. Yang, S. Ryu, and S. I. Seok, "Solvent engineering for high-performance inorganic-organic hybrid perovskite solar cells," *Nature Materials*, vol. 13, no. 9, pp. 897–903, 2014.

[99] G. E. Eperon, V. M. Burlakov, P. Docampo, A. Goriely, and H. J. Snaith, "Morphological control for high performance, solution-processed planar heterojunction perovskite solar cells," *Advanced Functional Materials*, vol. 24, no. 1, pp. 151–157, 2014.

[100] A. Dualeh, N. Tétreault, T. Moehl, P. Gao, M. K. Nazeeruddin, and M. Grätzel, "Effect of annealing temperature on film morphology of organic-inorganic hybrid pervoskite solid-state solar cells," *Advanced Functional Materials*, vol. 24, no. 21, pp. 3250–3258, 2014.

[101] M. Saliba, K. W. Tan, H. Sai et al., "Influence of thermal processing protocol upon the crystallization and photovoltaic performance of organic–inorganic lead trihalide perovskites," *Journal of Physical Chemistry C*, vol. 118, no. 30, pp. 17171–17177, 2014.

[102] L. Zheng, Y. Ma, S. Chu et al., "Improved light absorption and charge transport for perovskite solar cells with rough interfaces by sequential deposition," *Nanoscale*, vol. 6, no. 14, pp. 8171–8176, 2014.

[103] P. Docampo, F. C. Hanusch, S. D. Stranks et al., "Solution deposition-conversion for planar heterojunction mixed halide perovskite solar cells," *Advanced Energy Materials*, vol. 4, no. 14, Article ID 1400355, 2014.

[104] Y. Zhou, M. Yang, A. L. Vasiliev et al., "Growth control of compact $CH_3NH_3PbI_3$ thin films via enhanced solid-state precursor reaction for efficient planar perovskite solar cells," *Journal of Materials Chemistry A*, vol. 3, pp. 9249–9256, 2015.

[105] Y. Wu, A. Islam, X. Yang et al., "Retarding the crystallization of PbI2 for highly reproducible planar-structured perovskite solar cells via sequential deposition," *Energy and Environmental Science*, vol. 7, no. 9, pp. 2934–2938, 2014.

[106] Z. Xiao, C. Bi, Y. Shao et al., "Efficient, high yield perovskite photovoltaic devices grown by interdiffusion of solution-processed precursor stacking layers," *Energy & Environmental Science*, vol. 7, no. 8, pp. 2619–2623, 2014.

[107] Y. Deng, E. Peng, Y. Shao, Z. Xiao, Q. Dong, and J. Huang, "Scalable fabrication of efficient organolead trihalide perovskite solar cells with doctor-bladed active layers," *Energy and Environmental Science*, vol. 8, no. 5, pp. 1544–1550, 2015.

[108] K. M. Boopathi, M. Ramesh, P. Perumal et al., "Preparation of metal halide perovskite solar cells through a liquid droplet assisted method," *Journal of Materials Chemistry A*, vol. 3, no. 17, pp. 9257–9263, 2015.

[109] A. K. Chilvery, P. Guggilla, A. K. Batra, D. D. Gaikwad, and J. R. Currie, "Efficient planar perovskite solar cell by spray and brush solution-processing methods," *Journal of Photonics for Energy*, vol. 5, no. 1, 2015.

[110] G. Longo, L. Gil-Escrig, M. J. Degen, M. Sessolo, and H. J. Bolink, "Perovskite solar cells prepared by flash evaporation," *Chemical Communications*, vol. 51, no. 34, pp. 7376–7378, 2015.

[111] efficiency_chart.jpg (4190×2456), http://www.nrel.gov/ncpv/images/efficiency_chart.jpg.

[112] B. Ma, R. Gao, L. Wang et al., "Alternating assembly structure of the same dye and modification material in quasi-solid state dye-sensitized solar cell," *Journal of Photochemistry and Photobiology A: Chemistry*, vol. 202, no. 1, pp. 33–38, 2009.

[113] W. Li, J. Li, L. Wang, G. Niu, R. Gao, and Y. Qiu, "Post modification of perovskite sensitized solar cells by aluminum oxide for enhanced performance," *Journal of Materials Chemistry A*, vol. 1, no. 38, pp. 11735–11740, 2013.

[114] M. D. Kempe, A. A. Dameron, and M. O. Reese, "Evaluation of moisture ingress from the perimeter of photovoltaic modules," *Progress in Photovoltaics: Research and Applications*, vol. 22, no. 11, pp. 1159–1171, 2014.

[115] H.-S. Ko, J.-W. Lee, and N.-G. Park, "15.76% efficiency perovskite solar cells prepared under high relative humidity:

importance of PbI_2 morphology in two-step deposition of $CH_3NH_3PbI_3$," *Journal of Materials Chemistry A*, vol. 3, pp. 8808–8815, 2015.

[116] A. Fujishima, T. N. Rao, and D. A. Tryk, "Titanium dioxide photocatalysis," *Journal of Photochemistry and Photobiology C: Photochemistry Reviews*, vol. 1, no. 1, pp. 1–21, 2000.

[117] S. Ito, S. Tanaka, K. Manabe, and H. Nishino, "Effects of surface blocking layer of Sb_2S_3 on nanocrystalline TiO_2 for $CH_3NH_3PbI_3$ perovskite solar cells," *Journal of Physical Chemistry C*, vol. 118, no. 30, pp. 16995–17000, 2014.

[118] T. Leijtens, G. E. Eperon, S. Pathak, A. Abate, M. M. Lee, and H. J. Snaith, "Overcoming ultraviolet light instability of sensitized TiO_2 with meso-superstructured organometal trihalide perovskite solar cells," *Nature Communications*, vol. 4, article 2885, 2013.

[119] S. K. Pathak, A. Abate, T. Leijtens et al., "Towards long-term photostability of solid-state dye sensitized solar cells," *Advanced Energy Materials*, vol. 4, no. 8, Article ID 1301667, 2014.

[120] S. Guarnera, A. Abate, W. Zhang et al., "Improving the long-term stability of perovskite solar cells with a porous Al_2O_3 buffer layer," *The Journal of Physical Chemistry Letters*, vol. 6, no. 3, pp. 432–437, 2015.

[121] A. Poglitsch and D. Weber, "Dynamic disorder in methylammoniumtrihalogenoplumbates (II) observed by millimeter-wave spectroscopy," *The Journal of Chemical Physics*, vol. 87, no. 11, pp. 6373–6378, 1987.

[122] A. Dualeh, P. Gao, S. I. Seok, M. K. Nazeeruddin, and M. Grätzel, "Thermal behavior of methylammonium lead-trihalide perovskite photovoltaic light harvesters," *Chemistry of Materials*, vol. 26, no. 21, pp. 6160–6164, 2014.

[123] A. Pisoni, J. Jaćimović, O. S. Barišić et al., "Ultra-low thermal conductivity in organic-inorganic hybrid perovskite $CH_3NH_3PbI_3$," *Journal of Physical Chemistry Letters*, vol. 5, no. 14, pp. 2488–2492, 2014.

[124] S. N. Habisreutinger, T. Leijtens, G. E. Eperon, S. D. Stranks, R. J. Nicholas, and H. J. Snaith, "Carbon nanotube/polymer composites as a highly stable hole collection layer in perovskite solar cells," *Nano Letters*, vol. 14, no. 10, pp. 5561–5568, 2014.

[125] B. Hailegnaw, S. Kirmayer, E. Edri, G. Hodes, and D. Cahen, "Rain on methylammonium lead iodide based perovskites: possible environmental effects of perovskite solar cells," *The Journal of Physical Chemistry Letters*, vol. 6, no. 9, pp. 1543–1547, 2015.

[126] J. M. Frost, K. T. Butler, F. Brivio, C. H. Hendon, M. Van Schilfgaarde, and A. Walsh, "Atomistic origins of high-performance in hybrid halide perovskite solar cells," *Nano Letters*, vol. 14, no. 5, pp. 2584–2590, 2014.

[127] S. Liu, F. Zheng, N. Z. Koocher, H. Takenaka, F. Wang, and A. M. Rappe, "Ferroelectric domain wall induced band gap reduction and charge separation in organometal halide perovskites," *The Journal of Physical Chemistry Letters*, vol. 6, no. 4, pp. 693–699, 2015.

[128] E. L. Unger, E. T. Hoke, C. D. Bailie et al., "Hysteresis and transient behavior in current-voltage measurements of hybrid-perovskite absorber solar cells," *Energy and Environmental Science*, vol. 7, no. 11, pp. 3690–3698, 2014.

[129] H.-W. Chen, N. Sakai, M. Ikegami, and T. Miyasaka, "Emergence of hysteresis and transient ferroelectric response in organo-lead halide perovskite solar cells," *The Journal of Physical Chemistry Letters*, vol. 6, no. 1, pp. 164–169, 2015.

[130] J. Wei, Y. Zhao, H. Li et al., "Hysteresis analysis based on the ferroelectric effect in hybrid perovskite solar cells," *The Journal of Physical Chemistry Letters*, vol. 5, no. 21, pp. 3937–3945, 2014.

[131] H. J. Snaith, A. Abate, J. M. Ball et al., "Anomalous hysteresis in perovskite solar cells," *Journal of Physical Chemistry Letters*, vol. 5, no. 9, pp. 1511–1515, 2014.

[132] H.-S. Kim and N.-G. Park, "Parameters affecting I–V hysteresis of $CH_3NH_3PbI_3$ perovskite solar cells: effects of perovskite crystal size and mesoporous TiO_2 layer," *The Journal of Physical Chemistry Letters*, vol. 5, no. 17, pp. 2927–2934, 2014.

[133] A. Dualeh, T. Moehl, N. Tétreault et al., "Impedance spectroscopic analysis of lead iodide perovskite-sensitized solid-state solar cells," *ACS Nano*, vol. 8, no. 1, pp. 362–373, 2014.

[134] Y. Shao, Z. Xiao, C. Bi, Y. Yuan, and J. Huang, "Origin and elimination of photocurrent hysteresis by fullerene passivation in $CH_3NH_3PbI_3$ planar heterojunction solar cells," *Nature Communications*, vol. 2, p. 5748, 2014.

[135] C. C. Stoumpos, C. D. Malliakas, and M. G. Kanatzidis, "Semiconducting tin and lead iodide perovskites with organic cations: phase transitions, high mobilities, and near-infrared photoluminescent properties," *Inorganic Chemistry*, vol. 52, no. 15, pp. 9019–9038, 2013.

[136] Y. Kutes, L. Ye, Y. Zhou, S. Pang, B. D. Huey, and N. P. Padture, "Direct observation of ferroelectric domains in solution-processed $CH_3NH_3PbI_3$ perovskite thin films," *The Journal of Physical Chemistry Letters*, vol. 5, no. 19, pp. 3335–3339, 2014.

[137] Z. Xiao, Y. Yuan, Y. Shao et al., "Giant switchable photovoltaic effect in organometal trihalide perovskite devices," *Nature Materials*, 2014.

[138] B. Chen, J. Shi, X. Zheng et al., "Ferroelectric solar cells based on inorganic-organic hybrid perovskites," *Journal of Materials Chemistry A*, vol. 3, no. 15, pp. 7699–7705, 2015.

[139] H. J. Snaith, "Estimating the maximum attainable efficiency in dye-sensitized solar cells," *Advanced Functional Materials*, vol. 20, no. 1, pp. 13–19, 2010.

[140] M. A. Green, K. Emery, Y. Hishikawa, W. Warta, and E. D. Dunlop, "Solar cell efficiency tables (version 42)," *Progress in Photovoltaics: Research and Applications*, vol. 21, no. 5, pp. 827–837, 2013.

[141] P. K. Nayak, G. Garcia-Belmonte, A. Kahn, J. Bisquert, and D. Cahen, "Photovoltaic efficiency limits and material disorder," *Energy and Environmental Science*, vol. 5, no. 3, pp. 6022–6039, 2012.

[142] J. A. Christians, J. S. Manser, and P. V. Kamat, "Best practices in perovskite solar cell efficiency measurements. Avoiding the error of making bad cells look good," *The Journal of Physical Chemistry Letters*, vol. 6, pp. 852–857, 2015.

[143] J. H. Werner, R. Zapf-Gottwick, M. Koch, and K. Fischer, "Toxic substances in photovoltaic modules," in *Proceedings of the 21st International Photovoltaic Science and Engineering Conference*, Fukuoka, Japan, December 2011.

[144] N. K. Noel, S. D. Stranks, A. Abate et al., "Lead-free organic-inorganic tin halide perovskites for photovoltaic applications," *Energy and Environmental Science*, vol. 7, no. 9, pp. 3061–3068, 2014.

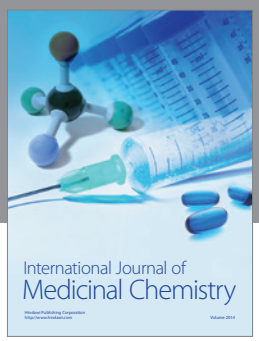

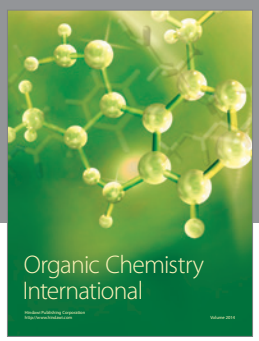

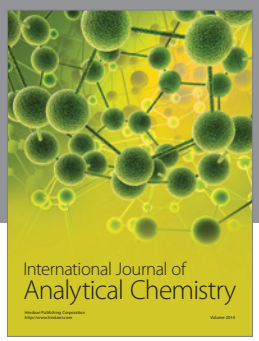

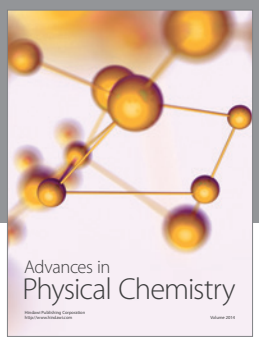

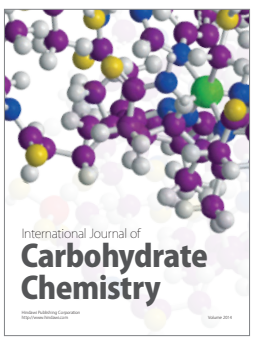

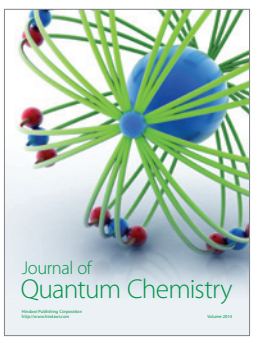

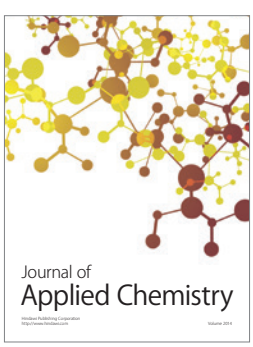

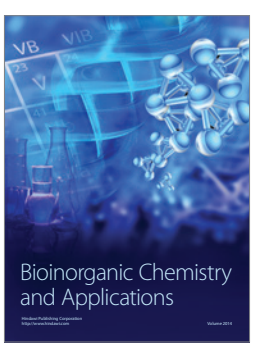

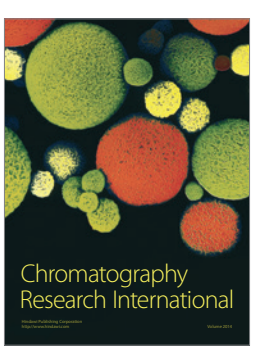

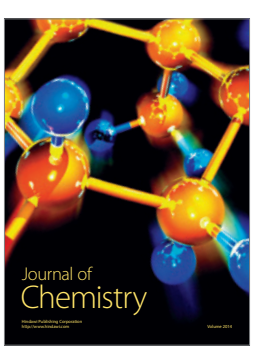

Hindawi

Submit your manuscripts at
http://www.hindawi.com